The electronic characterization of biphenylene—Experimental and theoretical insights from core and valence level spectroscopy

Johann Lüder, Monica de Simone, Roberta Totani, Marcello Coreno, Cesare Grazioli, Biplab Sanyal, Olle Eriksson, Barbara Brena, and Carla Puglia

Citation: The Journal of Chemical Physics **142**, 074305 (2015); doi: 10.1063/1.4907723
View online: http://dx.doi.org/10.1063/1.4907723
View Table of Contents: http://scitation.aip.org/content/aip/journal/jcp/142/7?ver=pdfcov
Published by the AIP Publishing

The electronic characterization of biphenylene—Experimental and theoretical insights from core and valence level spectroscopy

Johann Lüder,[1] Monica de Simone,[2] Roberta Totani,[3] Marcello Coreno,[4] Cesare Grazioli,[2,5] Biplab Sanyal,[1] Olle Eriksson,[1] Barbara Brena,[1] and Carla Puglia[1]
[1]*Department of Physics and Astronomy, Uppsala University, Box 516, SE-751 20 Uppsala, Sweden*
[2]*CNR-IOM, Laboratorio TASC, Sincrotrone Trieste, S.S. 14 Km 163.5, Basovizza, I-34149 Trieste, Italy*
[3]*Department of Physical and Chemical Sciences, University of l'Aquila, Via Vetoio, 67100 l'Aquila, Italy*
[4]*CNR-ISM, S.S. 14 Km 163.5, Basovizza, I-34149 Trieste, Italy*
[5]*Department of Chemical and Pharmaceutical Sciences, University of Trieste, 34127 Trieste, Italy*

(Received 26 October 2014; accepted 27 January 2015; published online 18 February 2015)

In this paper, we provide detailed insights into the electronic structure of the gas phase biphenylene molecule through core and valence spectroscopy. By comparing results of X-ray Photoelectron Spectroscopy (XPS) measurements with ΔSCF core-hole calculations in the framework of Density Functional Theory (DFT), we could decompose the characteristic contributions to the total spectra and assign them to non-equivalent carbon atoms. As a difference with similar molecules like biphenyl and naphthalene, an influence of the localized orbitals on the relative XPS shifts was found. The valence spectrum probed by photoelectron spectroscopy at a photon energy of 50 eV in conjunction with hybrid DFT calculations revealed the effects of the localization on the electronic states. Using the transition potential approach to simulate the X-ray absorption spectroscopy measurements, similar contributions from the non-equivalent carbon atoms were determined from the total spectrum, for which the slightly shifted individual components can explain the observed asymmetric features. © *2015 AIP Publishing LLC.* [http://dx.doi.org/10.1063/1.4907723]

I. INTRODUCTION

The biphenylene molecule ($C_{12}H_8$), shown in Fig. 1, is a polycyclic aromatic hydrocarbon (PAH) composed by two benzene rings connected by two bonds, forming a four-side ring. It can also be viewed as the conjunction of two benzyne molecules (C_6H_4), which are actually used for its synthesis. Biphenylene has been the target of several experimental and theoretical studies,[1,2] since it is very interesting both from the point of view of fundamental molecular physics and for its characteristic properties. For example, it can achieve anomalously high conductivity in a thin polyphthalidylidene biphenylene film.[3] Moreover, since it is the initial precursor of a 2D porous graphite-like molecular network called biphenylene carbon (BPC),[4] it is expected to play a major role as a novel organic material.

Although the electronic structure with 4π-electrons makes biphenylene an anti-aromatic molecule, according to the Hückel rules, the relatively long bond length between the two benzyne units weakens the interaction between them, giving biphenylene an intermediate character between anti-aromatic ring and aromatic ring.[5] Usually, the 4n π-electrons of anti-aromatic molecules have a more localized character with respect to the more delocalized 4n + 2 π electrons characteristic of aromatic molecules. As a consequence of this different electronic structure, the anti-aromatic molecules are characterized by an enhanced chemical reactivity, by lower stability[6] and often by interesting photo-physical properties. An example is the large vibrational progressions under photon-excitation[2] compared to other aromatic molecules.

Interestingly, biphenylene is one of the most stable anti-aromatic molecules making it very suitable for traditional spectroscopic experiments. The present study is the first characterisation of the electronic structure of the biphenylene molecule by means of soft X-ray spectroscopies. We provide a combined experimental and theoretical analysis of the core, valence, and unoccupied electronic states in the gas phase. The performed experimental measurements include X-ray Photoelectron Spectroscopy (XPS), valence Photoemission Spectroscopy (PES), and X-ray Absorption Spectroscopy (XAS). The theoretical analysis was performed by means of hybrid Density Functional Theory (DFT). The theory-experiment agreement obtained clarifies the atomic origin of the spectral features and in addition can give important information for the understanding of the electronic properties of functional materials formed by biphenylene building blocks. The article is organized as follows: after introducing the experimental and computational details of the various methods, first the results of the core electronic states are presented, then of the valence states, and last of the unoccupied electronic structure.

II. EXPERIMENTAL DETAILS

Photoelectron spectra and X-ray absorption spectra of biphenylene have been recorded at the GAs PHase (GAPH) beamline at the Elettra synchrotron, in Trieste.[7] Biphenylene is a solid powder at room temperature. It was purchased from Sigma-Aldrich (minimum purity of 99%, mp 113 C) and

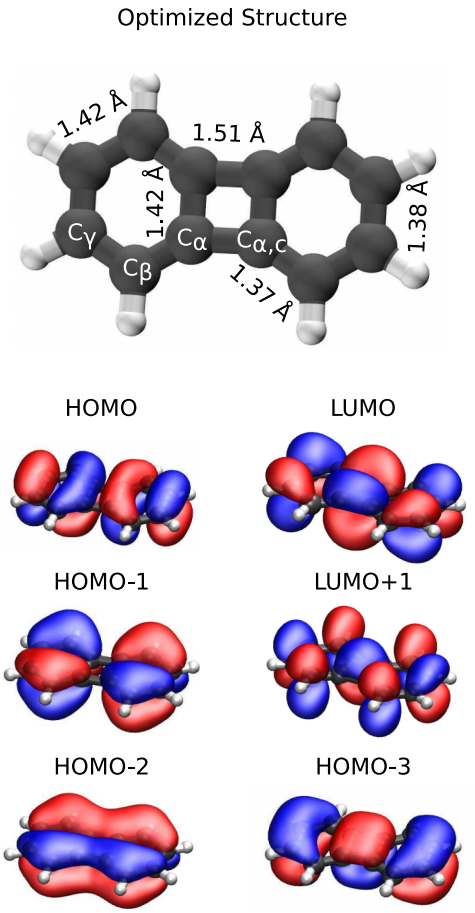

FIG. 1. B3LYP optimized structure of biphenylene. The bond lengths between the C atoms and the orbitals between HOMO-3 and LUMO+1 are given. All carbon atoms are gray and all hydrogen atoms are white. Orbitals are shown including their phases as red and blue isodensity surfaces.

introduced in the experimental chamber without further purification. The sample was sublimated using a custom built resistively heated furnace, based on a stainless steel crucible, a Thermocoax heating element, and a type K thermocouple. The spectra presented in the present work have been recorded at a working temperature of 85 C. The XPS and the PES data were recorded using a VG-Scienta SES-200 photoelectron analyzer[8] which was mounted at the magic angle of 54.7°. The use of this angle allows to record angle-integrated electron spectra. The valence band PES was recorded at a photon energy of 50 eV with an overall resolution of about 50 meV and it has been calibrated against the Xe $5p_{3/2,1/2}$ lines.[9] The C 1s spectrum has been recorded at a photon energy of 332 eV with an overall resolution of around 75 meV, and it has been calibrated against the C1s in CO_2 (297.6 eV).[10]

The photoabsorption spectra at the C K-edges were acquired with a photon energy resolution of 70 meV, by measuring the total ion yield (TIY) with a channel electron multiplier placed near the ionization region. The photon flux was measured simultaneously with a calibrated Si photodiode (AxVU100 IRD (TM)) for normalization purposes. The energy scale of the spectrum was calibrated by taking simultaneous spectra of the samples and of CO_2, with the characteristic transition at 290.77 eV (C 1s → π^*, CO2).[11,12]

III. COMPUTATIONAL DETAILS

The optimized molecular structure of biphenylene was obtained by means of DFT calculations using the GAUSSIAN 09 program[13] with the hybrid exchange-correlation functional Becke, 3-parameter, Lee-Yang-Parr (B3LYP).[14–17] The one-electron wave functions of biphenylene were described by the 6-311G(d,p) valence double ζ plus polarization basis sets[18] in the computation of the structure, while the eigenstate spectra were obtained by using the correlation-consistent polarized valence-only triples-zeta (cc-pVTZ) basis set[19] to increase accuracy of the electronic description. The PES of the valence band was compared to the eigenvalue spectrum of the relaxed molecule after the theoretical eigenvalues were convoluted with Gaussian functions to facilitate the comparison between theory and experiment. The Gaussian curves used in the convolution had a full width at half-maximum (FWHM) of 0.07 eV at eigenvalues higher than −10 eV, and it was increased linearly to 1.5 eV in the energy range from −10 to −32 eV. Below −32 eV, the broadening was kept constant again with a FWHM of 1.5 eV. The XPS and XAS spectra were simulated with the Stockholm-Berlin package StoBe,[20] which has been successfully employed for a variety of complex molecular systems including water,[21] phthalocyanines,[22] and adsorbed molecules.[23] The exchange and correlation effects of the many-electron system were approximated with the exchange functional by Becke[24] and the correlation functional by Perdew,[25] respectively, in the single particle picture in DFT. For the core ionized and the excited carbon atom, we used the igloo-III basis set by Kutzelnigg, Fleischer, and Schindler.[26]

The XPS spectra represent the binding energies of the core electrons. The C 1s XPS energies were calculated as the difference between the total energy of the molecule in the ground state and the total energy of the ionized molecule, where an electron has been removed from the 1s core level. The total C1s spectrum was aligned at the experimental energy scale. The comparison with the experimental results was done after the obtained energies were convoluted with a Gaussian curve with a FWHM of 70 meV. To estimate the influence of vibrational effects on the XPS measurements, the computed binding energies were convoluted with a skew Gaussian curve. In this way, we have approximated the asymmetric broadening of the XPS spectra due to vibrations, like in the XPS measurements of other small molecules.[27,28] Using the same FWHM of 70 meV, we have determined through the fitting procedure a skew factor α of 2.14. In detail, the convolution function $g_S(\epsilon)$ is given as

$$g_S(\epsilon) = Ne^{\left(\frac{-(\epsilon-E_{CH})^2}{(2\omega)^2}\right)} \int_{-\infty}^{\left(\alpha\frac{\epsilon-E_{CH}}{\omega}\right)} e^{\frac{-t^2}{2}} dt \qquad (1)$$

in which the usual Gaussian function centred at E_{CH} with the broadening σ is in the first part, N is the normalization factor, E_{CH} is the core hole binding energy, ω is the broadening factor, and α is the mentioned skew factor. This simple approach yielded good agreement with the experimental XPS spectrum by only taking the computed C1s binding energies for the three non-equivalent C atoms as input. The broadening was taken from experimental value of the FWHM of 70 meV. Although this procedure may provide a simple way to parametrize the effect of vibrational broadening on the XPS spectra, it cannot

account for high resolution XPS measurements revealing the detailed structures in the XPS data.

The C 1s XA spectra were computed with the Transition-Potential Approach (TPA),[29–31] implemented in the StoBe code[20] which has been successfully used for different molecules.[22,32,33] In a TPA calculation, the electronic relaxation effects induced by the transition of an electron from an initial 1s to a final state are simulated by introducing a half core-hole at the excited 1s core level. The transition probability is obtained as absolute square of the oscillator strengths calculated from the transition matrix elements between initial state and final state in the dipole approximation. To facilitate the comparison with the experiment, the transition intensities were convoluted with a Gaussian curve. The Gaussian had a FWHM of 0.4 eV below 287 eV; it was linearly increased from 0.4 to 2 eV in the energy range of 287 eV to 295 eV, and it was kept at 2 eV above 295 eV.

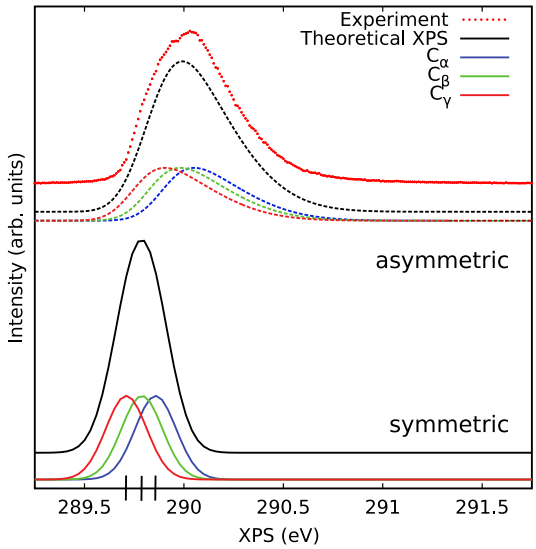

FIG. 2. Comparison between the experimental, dotted red curve, the theoretical XPS spectrum convoluted with Gaussian functions, solid curves, and with skew Gaussian functions dashed curves. The skew parameter α has been determined to be 2.14 by fitting to the experiment. Bars show explicitly the calculated XPS energies.

IV. RESULTS AND DISCUSSION

The B3LYP optimized structure of biphenylene is shown together with the intermolecular bond lengths in Fig. 1. The bond lengths obtained by DFT/B3LYP are in very close agreement with the experimental values,[1] see Table I, being in general just 0.01 Å shorter than the latter. Biphenylene is a flat molecule with three non-equivalent carbon atoms labelled as C_α, C_β, and C_γ. The C_α are the four C atoms that connect the two benzene rings to each other, as shown in Fig. 1. C_β and C_γ label the middle and the outer C atoms of the benzene rings, respectively. The computed distance between two C_γs is 1.39 Å. The bond lengths between the C_γ and the C_β as well as between C_α and C_β are slightly shorter of 1.37 Å. The distance between the two C_α in the same ring is 1.42 Å, while two connected C_α in different rings, indicated as C_α–$C_{\alpha,c}$ bond, have a bond length of 1.51 Å. The relative long bond distance between the C_α atoms of connected benzene rings is a consequence of the anti-aromatic character of the molecule.

The molecular orbitals (MOs) of the four highest occupied states, shown in Fig. 1, illustrate the spatial configuration and the localization/delocalization of the orbitals, as well as the character of the bonds, e.g., bonding, non-bonding, or anti-bonding. All depicted molecular orbitals are of π character and have in common a nodal plane in the molecular plane, while they differ in the locations and number of perpendicular nodal planes. The highest occupied molecular orbital (HOMO), for example, is composed by eight parts separated by perpendicular nodal planes which are located either between the connected benzene rings or along the C_β–C_γ bonds. The HOMO-2 has one longitudinally oriented nodal plane resulting in four orbital parts. This lengthwise plane is also present in LUMO and HOMO-1. A connection between the shown valence orbitals and the structural features can be easily drawn. HOMO and HOMO-1 have no bonding orbital between the connected rings, e.g., the C_α–$C_{\alpha,c}$ bond, weakening the bond which results in the elongated distance.

Core level spectroscopy is an element specific technique which provides insights into the chemical surrounding as well as chemical bonds of an atom in a molecule or solid. Fig. 2 compares the experimental XPS spectrum, red dotted curve, with the theoretical curves (solid and dashed lines) after convolution with the Gaussian and the skew Gaussian, respectively. Additionally, the spectra originated from the three non-equivalent carbon atoms are provided. The calculated XPS energies are shown as bars.

The experimental C1s spectrum consists of a large asymmetric peak with a FWHM of almost 0.5 eV at 290.1 eV. The XPS energies of the three chemically non-equivalent C atoms in biphenylene were calculated to be 289.82, 289.75, and 289.67 eV for the C_α, the C_β, and the C_γ, respectively, after alignment to the experimental spectrum. For molecules like naphthalene and biphenyl, comparable shifts in the 1s core levels have also been found for the carbon atoms connecting the two benzene-like rings.[27,28] After the fitting procedure including the skew parameter described above, the main experimental features could be reproduced.

The comparison of the XPS shifts can give valuable insights into the structural and chemical differences between

TABLE I. Comparison of the calculated B3LYP bond lengths in Å of biphenylene with available experimental crystallographic bond lengths provided in Ref. 1. $C_{\alpha,c}$ denotes a C_α of the connected benzyne ring.

	C_α–C_α	C_α–$C_{\alpha,c}$	C_α–C_β	C_β–C_γ	C_γ–C_γ
Experiment[1]	1.4294 (15)	1.5137 (15)	1.3786 (16)	1.4242 (16)	1.3913 (17)
B3LYP	1.4183	1.5065	1.3675	1.4153	1.3839

TABLE II. Relative C1s XPS shifts in eV among the non-equivalent C atoms in biphenylene, biphenyl, and naphthalene.

	$\Delta(C_\alpha - C_\gamma)$	$\Delta(C_{\beta_2} - C_\gamma)$	$\Delta(C_\beta - C_\gamma)$
Biphenylene (theory)	0.15		0.08
Biphenyl[a]	0.34	0.14	0.03
Naphthalene[b]	0.32		0.02

[a]Results taken from Ref. 27.
[b]Results taken from Ref. 28.

biphenylene and similar molecules composed of two benzene rings, here naphthalene and biphenyl, as can be seen in Table. II. We use here the convention of labelling the inner C atoms of the benzene ring as C_α, the outer C atoms as C_γ, and the C atoms between those two as C_β for biphenyl and naphthalene. This has the consequence that the biphenyl molecule has two non-equivalent C_β atoms, e.g., C_{β_1} and C_{β_2} that are connected to the C_α and the C_γ, respectively. Significant differences in the XPS shifts for biphenylene occur with respect to the naphthalene and biphenyl molecules. In detail, the $\Delta(C_\alpha - C_\gamma)$ shifts in the biphenylene molecule are about 0.17 eV smaller while $\Delta(C_\beta - C_\gamma)$ is larger for the biphenylene molecule and in between the shift seen in $\Delta(C_\beta - C_\gamma)$ and $\Delta(C_{\beta_2} - C_\gamma)$ for the biphenyl molecule. The latter shift indicates an accumulation of charge around the C_β which is supported by the ground state orbitals. These XPS shifts indicate some similarities in the electronic structure of these molecules. The bond between the two benzene rings in biphenylene is of different characters than the equivalent bonds in the biphenyl and in the naphthalene molecule. Also, the bonds between the C_β and the C_γ of the biphenylene molecule are more alike to the biphenyl molecule than to the naphthalene molecule. As discussed above, the anti-aromatic character of biphenylene causes distinct structural features and, in particular, it influences the bond lengths along the four-side rings. Consequently, this also affects the rest of the structure and causes a localisation of charge in each of the benzene rings centered at the C_β.

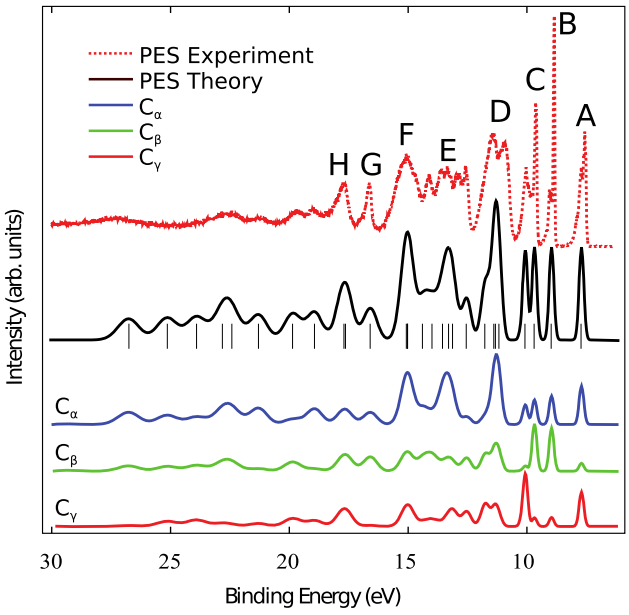

FIG. 3. Comparison between the experimental PES, dotted red curve, and the with B3LYP computed DOS and pDOSs. The total DOS is given as solid black curve together with the B3LYP eigenvalue spectrum indicated as bars below the DOS while the blue, the green, and the red curves represent the pDOSs from the C_α, the C_β, and the C_γ, respectively. The experimental binding energies are compared to the negative of the computed eigenvalues.

The valence spectra provide information about the highest energy occupied orbitals. The B3LYP eigenvalue spectrum is shown in Fig. 3 as solid black curve together with the experimental valence band photoelectron spectrum, red dotted curve, in a binding energy range between 3 and 21 eV. The peaks and group of peaks are labelled from A to H with A representing the HOMO. The solid black curve represents the total DOS obtained by the DFT calculation, which is the sum of the individual carbon contributions, e.g., C_α (blue curve), C_β (green curve), and C_γ (red curve), while the hydrogen contributions are not shown. The calculated spectra in Fig. 3 are shifted by 1.9 eV to match the experimental energies. The theoretical eigenvalues $-\epsilon$ and experimental binding energies E_{Bind} correspond approximately to the relation $-\epsilon_i = E_{Bind}$.

As in earlier studies for similar molecules,[33–35] B3LYP yields excellent agreement between experiment and theory. Especially, states between HOMO at 7.6 eV and below the HOMO until 10.5 eV are well reproduced. In this energy range, there are four eigenstates, which correspond to the four experimental peaks A to D, besides the small shoulders, which are due to vibrations.[27,28] Peak A, HOMO, has main contributions from the C_α and the C_γ atoms. Peak B, e.g., HOMO-1, is at 8.9 eV and has main contributions from the C_α and the C_β peaks. However, the correct intensity of the peak, almost twice as high in comparison to the HOMO peak, could not be reproduced in the calculations. HOMO-2 is at 9.7 eV and has main contributions from the C_α and the C_β atoms, while HOMO-3 at 10.0 eV has mainly contributions from the C_α and the C_γ atoms. At binding energies higher than 10.5 eV, vibrational effects increase the differences between theory and experiment. The group of peaks labelled with E are reproduced by B3LYP to some extent, but one particular peak at about 13 eV raising out of the group is not distinguishable to the same extent in the experiment. The origin of this extra-intense theoretical feature is connected to the pDOS of C_α atoms. The peaks F to H are well matched with the experiment even though peak F is slightly overestimated.

Interestingly, the electronic states of the peaks D to F are mostly represented by electrons from the C_α atoms, which form the square ring in biphenylene. In contrast, the states between HOMO and HOMO-3 consist of mixed contributions from at least two non-equivalent C atoms but always including the C_α atoms. This omnipresence of the C_α electronic states and the C_γ contributions to HOMO in the total DOS illustrate significant characteristics linked to the anti-aromaticity of biphenylene which may provide a promising starting point for studies aiming at modifying its properties through substitution of ligands or adsorption on surfaces as already performed for other planar molecules.[33,36–41]

The experimental and the theoretical XA spectra are shown in Fig. 4. The experimental curve is the red dotted curve. The total theoretical spectrum convoluted with the Gaussian function is the solid black curve, obtained as the sum of the contributions from the three non-equivalent carbon

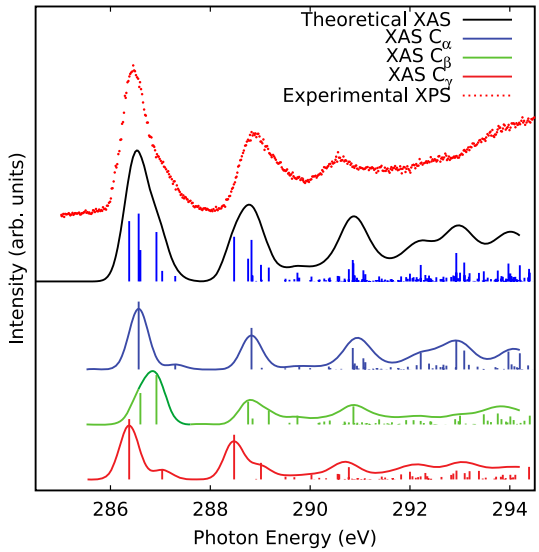

FIG. 4. The experimental XAS spectrum, dotted red curve, is compared to the results of the TPA approach. The total theoretical XAS spectrum is the solid black curve and the C atom contributions are the blue, the green, and the red curve for the C_α, the C_β, and the C_γ, respectively. The black bars below the total theoretical spectrum represent the absolute values of the dipole transition associated oscillator strengths.

atoms, C_α, C_β, and C_γ, the spectra of which are the blue, the green, and the red curves, respectively. Excellent agreement was achieved from the first excitation energy at 286.5 eV to the beginning of the continuum region at about 293 eV. The first experimental excitation peak at 286.5 eV has a broad shoulder towards higher energies and it is composed of contributions from all carbon atoms as shown by the calculations. However, the C_α and the C_γ contribute at about the same resonance energy of 286.5 eV and 286.6 eV, respectively, whereas the main contributions from the C_β is at a slightly higher energy (286.9 eV) resulting in a broadened feature in the total spectrum. The first resonance energies of the C_α and the C_γ are very similar to each other and their small variation in the energy position of 0.1 eV can be induced through symmetry breaking by the core-hole. The LUMO and LUMO + 1 have an energy difference of 0.4 eV in the ground state calculations and the same energy difference can be found on the transition to LUMO and LUMO + 1 in the TPA calculation. The contributions from C_β to these features are one order of magnitude smaller as from the other C atoms, which indicates that the C_β1s to LUMO + 1 transition is within the first peak at an energy of 286.9 eV. Moreover, the C_α and the C_γ have additional resonances between 286.9 eV and 287.4 eV which also contribute to the shoulder of the first experimental peak.

Similarly, the second peak at about 288.9 eV is also composed from contributions of all non-equivalent carbon atoms. In contrast to the first peak, the broadened feature is here composed of contributions from all C species, but the C_α and the C_γ atoms are the main contributors. Excellent agreement between theory and experiment was obtained for the energy difference of 2.4 eV between the first and the second peaks. The third experimental peak, consisting mainly of contributions from the C_α, at an energy position of 290.6 eV is slightly overestimated by 0.3 eV.

We have shown that the XAS peaks are composed from contributions of all non-equivalent carbons. The asymmetry of the first transitions could be explained with relative shift of the resonances of the non-equivalent carbon atoms which correspond to the computed XPS shift and are, therefore, caused by the different chemical bondings. These observations are expected also for these reasons for similar molecules like biphenyl and naphthalene.

The observed discrepancies among theoretical and experimental data could be due to various effects. For example, vibrational contributions could affect the spectra to spread various electronic contributions, minimizing the overlap between 1s and π^*-orbitals[42] as well as deformations of the molecular structure[6] as they can occur during excitation processes.

V. CONCLUDING REMARKS

We present a comprehensive study of the electronic structure of the biphenylene molecule by means of core- and valence level spectroscopy. The core level XPS and the XAS experiment could be reproduced with the full and the half core-hole approaches, respectively. All in all, the theoretical simulations show good agreement with the experimental results. The experimental valence PE spectrum is compared with the total DOS obtained from B3LYP calculations and the pDOS of the non-equivalent C atoms. The theoretical XA results, obtained in the TPA approach, show also very good agreement with the experimental result, considering the total theoretical XA spectrum as the sum of the contributions from the different C atoms.

In the future, it will be very interesting to study the interaction of biphenylene with substrates due to the growing technological interest in this and similar systems.[27,28] For such studies, it is important to have a theoretical tool with which to analyse experiments, in particular, to calculate spectral properties, and to have a means to reliably reproduce measurements. The results presented here are very encouraging in this regard, since they demonstrate that theory very accurately can reproduce observations and brings deepened understanding to the details of the measurements and the coupling between electronic structure and chemical bonds.

ACKNOWLEDGMENTS

J.L. is grateful to the Knut and Alice Wallenberg Foundation (KAW) for financial support. B.B. and C.P. acknowledge the Swedish Research Council (VR). We also acknowledge the Swedish National Infrastructure for Computing (SNIC) which has provided computing time on the clusters Abisko at Umeå University, Triolith at Linköping University, and Lindgren at KTH, Stockholm. We acknowledge the Carl Tygger Foundation, Sweden, for financial support and for making available the VG-Scienta SES-200 photoelectron analyser at the Gas Phase beamline, Elettra, Italy.

[1]T. C. W. Mak and J. Trotter, J. Chem. Soc. **1962**, 1.
[2]A. I. S. Holm, H. A. B. Johansson, H. Cederquist, and H. Zettergren, J. Chem. Phys. **134**, 044301 (2011).
[3]V. Zakrevskii, A. Ionov, and A. Lachinov, Tech. Phys. Lett. **24**, 539 (1998).

[4]G. Brunetto, P. A. S. Autreto, L. D. Machado, B. I. Santos, R. P. B. dos Santos, and D. S. Galvo, J. Phys. Chem. C **116**, 12810 (2012).
[5]M. E. Beck, R. Rebentisch, G. Hohlneicher, M. P. Fülscher, L. Serrano-Andrés, and B. O. Roos, J. Chem. Phys. **107**, 9464 (1997).
[6]R. Zimmermann, J. Mol. Struct. **377**, 35 (1996).
[7]K. C. Prince, R. R. Blyth, R. Delaunay, M. Zitnik, J. Krempasky, J. Slezak, R. Camilloni, L. Avaldi, M. Coreno, G. Stefani, C. Furlani, M. de Simone, and S. Stranges, J. Synchrotron Radiat. **5**, 565 (1998).
[8]N. Mårtensson, P. Baltzer, P. Brühwiler, J.-O. Forsell, A. Nilsson, A. Stenborg, and B. Wannberg, J. Electron Spectrosc. Relat. Phenom. **70**, 117 (1994).
[9]H.-H. Perkampus, Ber. Bunsengesellschaft Phys. Chem. **75**, 181 (1971).
[10]V. Myrseth, J. Bozek, E. Kukk, L. Sæthre, and T. Thomas, J. Electron Spectrosc. Relat. Phenom. **122**, 57 (2002).
[11]M. Tronc, G. C. King, and F. H. Read, J. Phys. B: At. Mol. Phys. **12**, 137 (1979).
[12]M. Tronc, G. C. King, and F. H. Read, J. Phys. B: At. Mol. Phys. **13**, 999 (1980).
[13]M. J. Frisch, G. W. Trucks, H. B. Schlegel, G. E. Scuseria, M. A. Robb, J. R. Cheeseman, G. Scalmani, V. Barone, B. Mennucci, G. A. Petersson, H. Nakatsuji, M. Caricato, X. Li, H. P. Hratchian, A. F. Izmaylov, J. Bloino, G. Zheng, J. L. Sonnenberg, M. Hada, M. Ehara, K. Toyota, R. Fukuda, J. Hasegawa, M. Ishida, T. Nakajima, Y. Honda, O. Kitao, H. Nakai, T. Vreven, J. A. Montgomery, Jr., J. E. Peralta, F. Ogliaro, M. Bearpark, J. J. Heyd, E. Brothers, K. N. Kudin, V. N. Staroverov, R. Kobayashi, J. Normand, K. Raghavachari, A. Rendell, J. C. Burant, S. S. Iyengar, J. Tomasi, M. Cossi, N. Rega, J. M. Millam, M. Klene, J. E. Knox, J. B. Cross, V. Bakken, C. Adamo, J. Jaramillo, R. Gomperts, R. E. Stratmann, O. Yazyev, A. J. Austin, R. Cammi, C. Pomelli, J. W. Ochterski, R. L. Martin, K. Morokuma, V. G. Zakrzewski, G. A. Voth, P. Salvador, J. J. Dannenberg, S. Dapprich, A. D. Daniels, C3. Farkas, J. B. Foresman, J. V. Ortiz, J. Cioslowski, and D. J. Fox, GAUSSIAN 09 REVISION C.01, GAUSSIAN INC., WALLINGFORD, CT, 2009.
[14]P. Stephens, F. Devlin, C. Chabalowski, and M. J. Frisch, J. Phys. Chem. **98**, 11623 (1994).
[15]S. Vosko, L. Wilk, and M. Nusair, Can. J. Phys. **58**, 1200 (1980).
[16]C. Lee, W. Yang, and R. Parr, Phys. Rev. B **37**, 785 (1988).
[17]A. D. Becke, J. Chem. Phys. **98**, 1372 (1993).
[18]A. D. McLean and G. S. Chandler, J. Chem. Phys. **72**, 5639 (1980).
[19]R. A. Kendall, T. H. Dunning, and R. J. Harrison, J. Chem. Phys. **96**, 6796 (1992).
[20]StoBe-deMon version 3.3, 2014, K. Hermann and L. G. M. Pettersson, M. E. Casida, C. Daul, A. Goursot, A. Koester, E. Proynov, A. St-Amant, and D. R. Salahub. Contributing authors: V. Carravetta, H. Duarte, C. Friedrich, N. Godbout, M. Gruber, J. Guan, C. Jamorski, M. Leboeuf, M. Leetmaa, M. Nyberg, S. Patchkovskii, L. Pedocchi, F. Sim, L. Triguero, and A. Vela.
[21]H. Ogasawara, B. Brena, D. Nordlund, M. Nyberg, A. Pelmenschikov, L. G. M. Pettersson, and A. Nilsson, Phys. Rev. Lett. **89**, 276102 (2002).
[22]M.-N. Shariati, J. Lüder, I. Bidermane, S. Ahmadi, E. Göthelid, P. Palmgren, B. Sanyal, O. Eriksson, M. N. Piancastelli, B. Brena *et al.*, J. Phys. Chem. C **117**, 7018 (2013).
[23]D. Klar, B. Brena, H. C. Herper, S. Bhandary, C. Weis, B. Krumme, C. Schmitz-Antoniak, B. Sanyal, O. Eriksson, and H. Wende, Phys. Rev. B **88**, 224424 (2013).
[24]A. D. Becke, Phys. Rev. A **38**, 3098 (1988).
[25]J. P. Perdew, Phys. Rev. B **33**, 8822 (1986).
[26]W. Kutzelnigg, U. Fleischer, and M. Schindler, "The IGLO-method: *Ab-Initio* calculation and interpretation of NMR chemical shifts and magnetic susceptibilities," in *NMR Basic Principles and Progress* (Springer Verlag, Berlin, Heidelberg, 1991), pp. 165–262.
[27]I. Minkov, F. Gel'mukhano, H. Ågren, R. Friedlein, C. Suess, and W. R. Salaneck, J. Phys. Chem. A **109**, 1330 (2005).
[28]I. Minkov, F. Gelmukhanov, R. Friedlein, W. Osikowicz, C. Suess, G. Öhrwall, S. L. Sorensen, S. Braun, R. Murdey, W. R. Salaneck, and H. Ågren, J. Chem. Phys. **121**, 5733 (2004).
[29]J. C. Slater, Adv. Quantum Chem. **6**, 1 (1972).
[30]J. C. Slater and K. H. Johnsson, Phys. Rev. B **5**, 844 (1972).
[31]L. Triguero, Y. Luo, L. G. M. Pettersson, H. Ågren, P. Väterlein, M. Weinelt, A. Föhlisch, J. Hasselström, O. Karis, and A. Nilsson, Phys. Rev. B **59**, 5189 (1999).
[32]M. Nyberg, Y. Luo, L. Triguero, L. G. M. Pettersson, and H. Ågren, Phys. Rev. B **60**, 7956 (1999).
[33]I. Bidermane, J. Lüder, S. Boudet, T. Zhang, S. Ahmadi, C. Grazioli, M. Bouvet, J. Rusz, B. Sanyal, O. Eriksson *et al.*, J. Chem. Phys. **138**, 234701 (2013).
[34]I. E. Brumboiu, R. Totani, M. de Simone, M. Coreno, C. Grazioli, L. Lozzi, H. C. Herper, B. Sanyal, O. Eriksson, C. Puglia, and B. Brena, J. Phys. Chem. A **118**, 927 (2014).
[35]B. Brena, C. Puglia, M. de Simone, M. Coreno, K. Tarafder, V. Feyer, R. Banerjee, E. Gthelid, B. Sanyal, P. M. Oppeneer, and O. Eriksson, J. Chem. Phys. **134**, 074312 (2011).
[36]J. Lüder, B. Sanyal, O. Eriksson, C. Puglia, and B. Brena, Phys. Rev. B **89**, 045416 (2014).
[37]S. M. Yoon, S. J. Lou, S. Loser, J. Smith, L. X. Chen, A. Facchetti, and T. Marks, Nano Lett. **12**, 6315 (2012).
[38]B. Chilukuri, U. Mazur, and K. W. Hipps, Phys. Chem. Chem. Phys. **16**, 14096 (2014).
[39]J. Lüder, O. Eriksson, B. Sanyal, and B. Brena, J. Chem. Phys. **140**, 124711 (2014).
[40]M. Garvey, J. Kestell, R. Abuflaha, D. W. Bennett, G. Henkelman, and W. T. Tysoe, J. Phys. Chem. C **118**, 20899 (2014).
[41]M. Iannuzzi, F. Tran, R. Widmer, T. Dienel, K. Radican, Y. Ding, J. Hutter, and O. Groning, Phys. Chem. Chem. Phys. **16**, 12374 (2014).
[42]G. Fronzoni, O. Baseggio, M. Stener, W. Hua, G. Tian, Y. Luo, B. Apicella, M. Alfé, M. de Simone, A. Kivimäki, and M. Coreno, J. Chem. Phys. **141**, 044313 (2014).